l- and n-changing collisions during interaction of a pulsed beam of Li Rydberg atoms with CO_2

B. Dubreuil and M. Harnafi
Groupe de Recherche sur l'Energétique des Milieux Ionisés, Université d'Orléans, Boîte Postale No. 6759, 45067 Orleans CEDEX 2, France
(Received 9 January 1989)

The pulsed Li atomic beam produced in our experiment is based on controlled transversely-excited-atmospheric CO_2 laser–induced ablation of a Li metal target. The atomic beam is propagated in vacuum or in CO_2 gas at low pressure. Atoms in the beam are probed by laser-induced fluorescence spectroscopy. This allows the determination of time-of-flight and velocity distributions. Li Rydberg states ($n=5-13$) are populated in the beam by two-step pulsed-laser excitation. The excited atoms interact with CO_2 molecules. l- and n-changing cross sections are deduced from the time evolution of the resonant or collision-induced fluorescence following this selective excitation. l-changing cross sections of the order of 10^4 Å^2 are measured; they increase with n as opposed to the plateau observed for Li* colliding with a diatomic molecule. This behavior is qualitatively well explained in the framework of the free-electron model. $n \rightarrow n'$ changing processes with large cross sections (10–100 Å^2) are also observed even in the case of large electronic energy change ($\Delta E_{nn'} > 10^3$ cm^{-1}). These results can be interpreted in terms of resonant-electronic to vibrational energy transfers between Li Rydberg states and CO_2 vibrational modes.

I. INTRODUCTION

Molecular rotational and electronic energies can be exchanged during a collision of a Rydberg atom with a molecule, leading to resonant l- and n-changing processes characterized by large cross sections.[1–3] The study of such mechanisms for Li($n\,^2D$) excited states was reported three years ago by Dubreuil and Harnafi in the case of H_2 and D_2 interactions.[2] In this experiment, Li atoms were produced in a heat-pipe oven. Exchange of electronic to rotational energy with $\Delta J=2$ was observed.

These resonant transfers are rather well described by e^--quadrupole interaction.[4] For example, the 7.7 Å^2 theoretical cross section for the collision

$$\mathrm{Li}(n=10)+\mathrm{H_2}(J=1)\rightarrow \mathrm{Li}(n=8)+\mathrm{H_2}(J=3)+27\ \mathrm{cm^{-1}}$$

is in excellent agreement with our measurements. In the course of these previous experiments, we attempted also to study collisions of Li Rydberg states with CO_2 molecules, but the strong reactivity of CO_2 with Li in the cell prevented us from performing reliable measurements. This difficulty is now avoided by the use of a pulsed Li atomic beam produced by the controlled laser ablation of a solid Li target. In this way, the Li atoms are renewed in every laser shot.

By combining this technique with time-resolved laser-induced fluorescence (LIF) spectroscopy, and following the procedure previously developed for the cell experiments,[2,5] we are able to deduce cross sections for the l-mixing quasielastic collisions of the type

$$\mathrm{Li}(n\,^2D)+\mathrm{CO_2}\rightarrow \mathrm{Li}(n\,^2L,\ L\geq 3)+\mathrm{CO_2}\ , \qquad (1)$$

where $n=5-13$, and also for the inelastic n-changing collisions of the type

$$\mathrm{Li}(n)+\mathrm{CO_2}\rightarrow \mathrm{Li}(n')+\mathrm{CO_2}+\Delta E_{nn'}\ . \qquad (2)$$

Large cross sections (10–100 Å^2) are measured for process (2) with $n'<n$ even for large energy change of the Rydberg electron ($\Delta E_{nn'} > 1000$ cm^{-1}). As for H_2 and D_2, such large cross sections are probably associated with resonant transfers, the electronic energy released by the atom being transferred to an internal excitation mode of the molecule. However, for CO_2, rotational transfers cannot account for the observed present results because of the large energy exchanged during the collision.

In fact, large $n \rightarrow n'$ transfer cross sections are obtained when $\Delta E_{nn'}$ is closed to the energy of a vibrational infrared or Raman transition starting from the CO_2 ground state. This suggests that resonant-electronic to vibrational energy transfer is a possible mechanism[6] to interpret the variation of the n-changing cross sections with $\Delta E_{nn'}$.

II. EXPERIMENT

A. Experimental setup

The general experimental arrangement is shown in Fig. 1. It is composed of two main parts: the Li atomic beam production and the LIF measurement systems. The latter is essentially the same as was developed for our previous cell experiments.[2,5]

1. Li atomic beam

The pulsed Li atomic beam is produced by laser ablation of a solid Li target. Detailed studies on the ablation processes are reported elsewhere,[7] and in the following, only the part relevant to the collision experiment will be described.

 ©1989 The American Physical Society

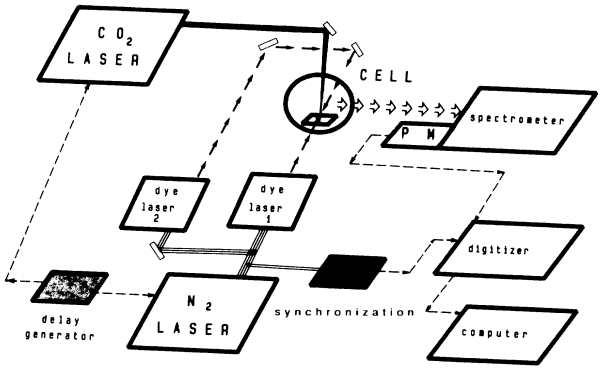

FIG. 1. Experimental setup.

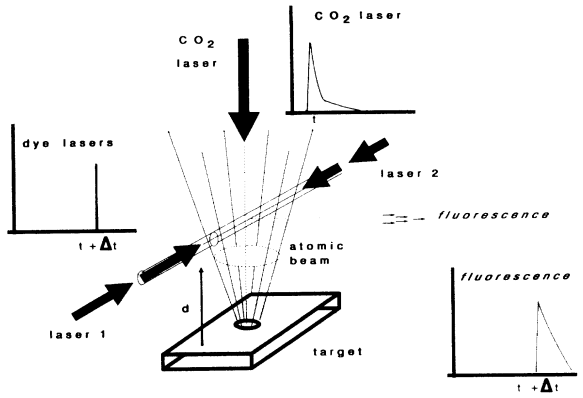

FIG. 2. Geometry of the laser–atomic-beam interaction. The CO_2 laser fired at time t is the ablating laser. Lasers 1 and 2 probe the atomic beam at the time $t+\Delta t$ and at a distance d from the surface. The resulting laser-induced fluorescence (LIF) is recorded.

The method is based on front surface illumination of the metal target with relatively low-energy laser pulses. This approach is similar to that in the works of Leismann *et al.*[8] and Dreyfus *et al.*[9] The cell is composed of a vacuum vessel evacuated to a residual pressure of 0.5×10^{-7} Torr. CO_2 gas can be introduced at precisely controlled pressure in the range 10^{-4}–10^{-1} Torr. The results reported here were obtained for CO_2 pressures up to 2×10^{-2} Torr. The Li metal target is positioned inside the cell and is irradiated perpendicularly to its surface by the beam of a GENTEC DD-250 transversely-excited-atmospheric (TEA) CO_2 laser working at 10 Hz. After spatial filtering and attenuation, the infrared ($\lambda=10.6$ μm) beam is focused on the surface to a spot size of 2 mm in diameter. Taking into account spatial reduction and attenuation, we estimate that the laser energy on the surface is typically of the order of 5 mJ. However, most of the laser energy is in fact reflected and only a few percent is absorbed. The main part of this energy is contained in a pulse of 150-ns duration. Under these conditions, no plasma is formed on the surface, and only a fraction of a Li monolayer is ablated during each laser shot. This results in a pulsed atomic beam which is relatively well reproducible.

Atoms in the beam of ablated material are probed by time-resolved LIF. These measurements are performed by varying the delay time between the CO_2 laser shot and the N_2-pumped pulsed dye lasers used to probe the ablated neutral atoms. Such measurements are carried out at various distances from the target surface as depicted in Fig. 2. This allows the determination of time-of-flight distribution of the atomic beam with good time resolution ($\sim$20 ns). For example, Fig. 3 shows the temporal evolution of the relative density of Li atoms as deduced from the two-step laser excitation of the $7\,^2D$ state at 5 and 15 mm from the target surface in vacuum. The mean beam velocity v deduced from the displacement of the maximum is 3.8×10^5 cm/s.

Detailed studies[7] indicate that the time-of-flight distributions can be relatively well described by Maxwell functions except for the early times for which the finite duration of the ablating laser pulse must be taken into account. Such measurements were also performed in the presence of low gas pressure in the cell. The shape of the distribution and $\bar{v}$ are practically unaffected by diffusion as long as $P_{co_2}<2\times10^{-2}$ Torr. Absolute atom-density calibration is deduced from laser absorption on the Li $2S$-$2P$ transition. In this case, the broad line profile (0.8 Å) of the probe beam at 6707 Å is recorded at the output of the cell by a gated optical multichannel analyzer (EGG OMA III) connected to the spectrometer.

The atom density is determined from the absorption profile, the absorption length being measured by imaging the LIF emitted by the probed atoms with a charge coupled device camera. In the conditions of the present experiment the mean density at a distance $d=15$ mm from the surface is of the order of 10^{11} cm^{-3}. This corresponds to about 2×10^{11} atoms ablated per laser shot. This value is sufficiently low to ensure good reproducibility of the laser-surface interaction and to avoid Li*-Li collisional interactions within the atom beam.

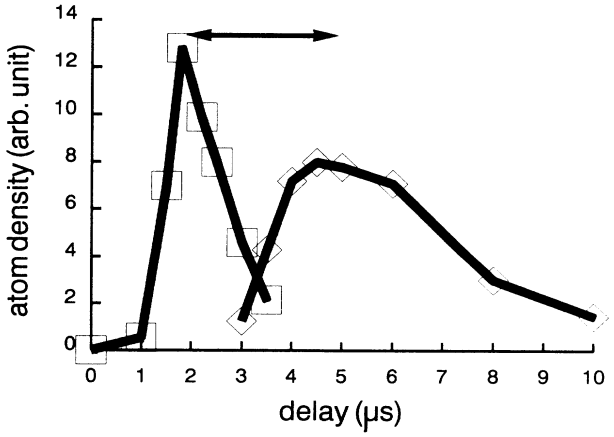

FIG. 3. Time-of-flight distribution of the $7\,^2D$ Li excited states in the beam for two distances from the surface: □, $d=5$ mm; ◇, $d=15$ mm. The arrow indicates the time shift of the maximum of the distribution. The mean beam velocity $\bar{v}=3.8\pm0.8\times10^5$ cm/s is deduced from this shift.

TABLE I. Measured l-mixing cross sections in units of 10^{-13} cm^2. The numbers in parentheses represent the experimental uncertainties.

Target	n 5	6	7	8	9	10	11	12	13
CO[a]		1.3(0.2)	2.0(0.3)	1.8(0.3)	1.5(0.3)	1.3(0.2)	1.0(0.2)	1.3(0.3)	1.1(0.2)
H_2[b]		0.7(0.1)	1.7(0.3)	1.1(0.3)	1.1(0.1)	1.1(0.1)	1.2(0.1)	1.2(0.1)	1.2(0.1)
CO_2[c]	1.5(0.6)	2.8(1.1)	5.5(2.2)	13(5)	10(4)	8(3)	14(5)	16(6)	17(6)

[a]Reference 5, collision velocity $\bar{v}=1.55\times10^5$ cm/s.
[b]Reference 5, $\bar{v}=3\times10^5$ cm/s.
[c]$\bar{v}=3.8\times10^5$ cm/s.

2. *Excitation of the Li atoms: Collision experiment*

As in our previous work,[2,5] Li($n\,^2D$) states are populated by two-step pulsed-laser excitation. The two dye laser beams (0.5 mm diameter, energy ~0.5 μJ/pulse are propagated collinearly in opposite directions and cross the atomic beam at a distance $d=15$ mm from the surface (see Fig. 2). They are simultaneously fired at the time corresponding to the maximum of the time-of-flight distribution. The velocity of the probed atoms is then $\bar{v}=(3.8\pm0.8)\times10^5$ cm/s. (Note that by varying the delay between the ablating laser and the probe laser, different velocity classes can in principle be probed by this method.) The excitation and relaxation of the $n\,^2D$ population is monitored by the time-resolved $n\,^2D\rightarrow2\,^2P$ resonance fluorescence detected with a spectrometer and a photomultiplier connected to a 200-MHz digitizer (Tektronix 7912 AD). The fluorescence emitted by the $n'\,^2D$ states ($n'\neq n$) serves as a probe of the n-changing processes [Eq. (2)]. More particularly, the Li($n\,^2D$)–CO_2 collision cross sections are deduced from the analysis of the time evolution of the resonance and collision-induced LIF signals as a function of the CO_2 pressure in the cell.

III. RESULTS AND DISCUSSION

A. *l*-mixing processes

The $n\,^2D\rightarrow2\,^2P$ resonance-fluorescence signals exhibit a two-exponential decay typical of the collisional coupling of the $n\,^2D$ state with the nearly degenerate $n\,^2L$ ($L>2$) states [Eq. (1)].

As explained in Refs. 2, 5, and 10, the rate coefficient $k_{l_{\rm mix}}$ of the l-mixing process can be deduced from the variation of the slope of the fast component versus CO_2 pressure. The l-mixing cross sections $\sigma_{l_{\rm max}}=k_{l_{\rm mix}}/\bar{v}$ are given in Table I for $n=5$–13 and compared to those obtained with CO and H_2.[2] We assume here that the Li-CO_2 mean collision velocity is given by the propagation velocity of the Li atomic beam in the CO_2 gas target. This is certainly a good approximation, considering the relatively low thermal velocity of CO_2 at $T=300$ K ($\sim10^5$ cm/s).

Table I shows that the Li($n\,^2D$)–CO_2 l-mixing cross sections are about one order of magnitude larger than for CO and H_2. Furthermore, they increase with n, whereas a broad maximum around $n=7$–8 was observed for the diatomic molecules.[2] These differences can be explained qualitatively in terms of free-electron–molecule interaction as proposed for other l-mixing processes. As shown by Hickman,[11] in this scheme $\sigma_{l_{\rm mix}}$ is a product of three factors: the geometrical factor (n^4 scaling), the probability that a CO_2 molecule will encounter the Rydberg electron (increases with the e^--CO_2 scattering cross section and decreases with n), and the probability that the quasielastic collision will cause a transition into a different quantum state (depends on the energy gap).

As reported in Ref. 12, the momentum-transfer cross sections for collisions of electrons with CO_2 [electron energy $=1/(2n^2)$] increase strongly with n in the range of interest, whereas they stay approximately constant for CO, N_2, and H_2. This increase largely compensates for the decrease of the probability of the collision event with n. Figure 4 compares the scaling formula of Hickman to

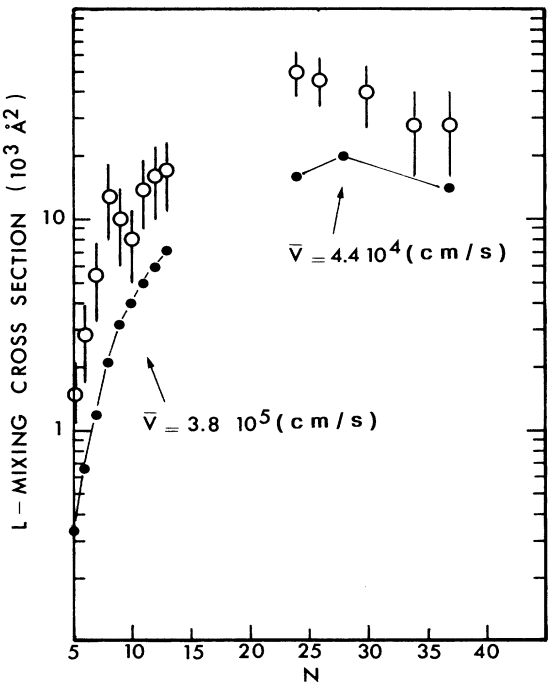

FIG. 4. l-mixing cross sections for CO_2–Rydberg-state collisions as a function of the principal quantum number n. Φ, experimental results: $n=5$–13, Li-CO_2 collisions, $\bar{v}=3.8\times10^5$ cm/s (this work); $n=25$–37, Xe-CO_2 collisions (Higgs *et al.*, Ref. 13); ●, theoretical values deduced from the scaling formula of Hickman (Ref. 11).

our cross sections ($n=5-13$) and also to those of Higgs *et al.*[13] obtained for Xe(nf)-CO_2 collisions ($n=24-37$). It can be seen that the n dependence is well reproduced by the theory over the whole n range. In Ref. 13 the mean Xe-CO_2 collision velocity was $\bar{v}\sim 4\times 10^4$ cm/s; scaling the results to $\bar{v}\sim 3.8\times 10^5$ cm/s will slightly decrease the measured cross section because the probability that CO_2 will encounter the Rydberg electron decreases when $\bar{v}$ increases.

While there is good overall agreement, we note that the absolute theoretical values are systematically lower than the experimental data. This difference can probably be ascribed to the fact that the CO_2 molecule is not a sphere contrary to what is assumed in the model of Hickman and can interact with the Rydberg states with particular orientations.

B. n-changing processes

n-changing processes are studied using the method developed for the diatomic molecule collisions.[2] The time-resolved fluorescence intensities starting from the $(n\pm 1)$, $(n\pm 2)^2D$ levels are measured when the $n\,^2D$ state ($n=6,9,10$) is laser excited. These processes dominate the late time evolution of the populations after the time t_0 for which l mixing is completely achieved.[2,10] In this time period, all the quantum substates of a given n (except probably the $n\,^2S$ states) are populated and contribute with the same probability to the $n\rightarrow n'$ transfer. After calibration of the detection system, the rate coefficients $k_{n-n'}$ and the corresponding cross sections $\sigma_{n-n'}$ are deduced from the measurements of the integrated LIF signals and the values of the slope of the slow component of the resonant-fluorescence signal (quenching rate of the n manifold) for different CO_2 pressures.

The cross sections for the $10\rightarrow 9$, $10\rightarrow 8$, $9\rightarrow 8$, $9\rightarrow 7$, $6\rightarrow 5$, and $6\rightarrow 4$ transfers are shown in Fig. 5 as a function of the change in the Rydberg atoms energy $\Delta E_{nn'}=|E_n-E_{n'}|$ assuming hydrogenic levels. In fact, only $n'<n$ transfers could be observed with measurable cross sections. Their values for $\Delta E_{nn'}<1500$ cm^{-1} are one order of magnitude larger than in the H_2 or D_2 collision experiments. Evidence for energy transfer with $\Delta E_{nn'}$ as large as 3800 cm^{-1} with a cross section of 20 Å has been obtained.

Quite generally, such large cross-section values are the earmark of a resonant process. Indeed, the theoretical estimates for the inelastic nonresonant processes [Eq. (2)] deduced from the work of Petitjean and Gounand[4] and shown in Fig. 4 exhibit a rapid decay of the cross section σ^{in} when $\Delta E_{nn'}$ increases. σ^{in} falls down 1 Å^2 for $\Delta E_{nn'}$ greater than 800 cm^{-1}.

Resonant-electronic to purely rotational energy transfer, such as has been observed in H_2 and D_2 collisions,[2] cannot occur in CO_2 since the large observed $\Delta E_{nn'}$ values are not compatible with the low CO_2 rotational constant (~ 0.3 cm^{-1}). Instead, the order of magnitude of observed $\Delta E_{nn'}$ values suggests vibrational excitation transfers may be involved. The energies of the first vibrational states of CO_2 are indicated on the energy axis in Fig. 5. The indicated excited vibrational states are

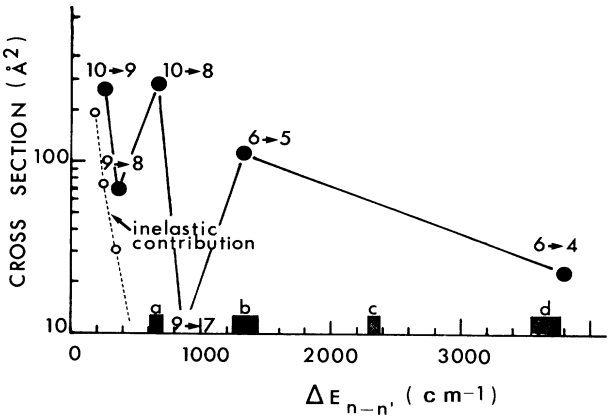

FIG. 5. n-n' changing cross sections for collisions of Li(n) with CO_2 as a function of the energy change $\Delta E_{n-n'}$. On the energy axis are indicated the positions of the first ir and Raman transitions in CO_2 (see Ref. 14 for notations). *a*, ir $\Sigma_g^+(00^00)\rightarrow\pi_u(01^10)$; *b*, Raman $\Sigma_g^+(00^00)\rightarrow\Sigma_g^+(02^00)$, $\Sigma_g^+(00^00)\rightarrow\Sigma_g^+(10^00)$; *c*, ir $\Sigma_g^+(00^00)\rightarrow\Sigma_u^+(00^01)$; *d*, ir $\Sigma_g^+(00^00)\rightarrow\Sigma_g^+(02^01)$, $\Sigma_g^+(00^00)\rightarrow\Sigma_g^+(10^01)$.

connected to the ground state through strong infrared and Raman transitions. The corresponding center frequencies and bandwidths are given in Table II using the data of Ref. 14.

From Fig. 4 it is clear that the $10\rightarrow 9$ and $9\rightarrow 8$ transfers correspond to the inelastic n-changing process [Eq. (2)] without vibrational excitation: the corresponding $\Delta E_{nn'}$ values do not exceed 400 cm^{-1} and their cross sections follow roughly the theoretical prediction. The same holds no doubt for the $9\rightarrow 7$ transfer with $\Delta E_{nn'}=885$ cm^{-1} which could not be detected. By contrast, the sharp structures of the $10\rightarrow 8$, $6\rightarrow 5$, and $6\rightarrow 4$ transfers correspond to an electronic energy change in near coincidence with the energies of the CO_2 infrared or Raman transitions (see Table II). This fact and the large values of the corresponding cross sections suggest that the following resonant or near-resonant energy-transfer processes may be responsible for the observed n-changing processes:

$$\text{Li}(n)+\text{CO}_2(n_1,n_2,n_3)\rightarrow\text{Li}(n')+\text{CO}_2(n_1',n_2',n_3')+\delta$$

n	(n_1,n_2,n_3)	n'	(n_1',n_2',n_3')
10	(0,0,0)	(8)	(0,1,0)
6	(0,0,0)	(5)	(0,2,0) and (1,0,0)
6	(0,0,0)	(4)	(0,2,1) and (1,0,1)

where n_1, n_2, and n_3 (n_1', n_2', and n_3', respectively) are the vibrational quantum numbers of the CO_2 molecule and δ is the energy detuning from resonance.

It is interesting to note that the measured cross sections for these three processes follow roughly the magnitude of the corresponding ir or Raman transitions, that is, the magnitude of the vibrational transition matrix elements. Furthermore, the lowest cross section obtained for the $6\rightarrow 4$ transfer corresponds to the largest detuning from resonance (~ 100 cm^{-1}). This is consistent with a resonant process whose cross section is[4] the product of the square of the vibrational transition moment

TABLE II. Energies of the vibrational transitions in CO_2 and n-changing processes in Li.

Li n-changing transition $n \rightarrow n'$	Energy charge $\Delta E_{nn'}$ (cm^{-1})	CO_2 vibrational transitions transition	nature	center frequency (cm^{-1})	width (cm^{-1})
$10 \rightarrow 8$	618 cm^{-1}	$\Sigma_g^+(0^00) \rightarrow \Pi_u(01^10)$	ir very strong	667.3	~ 60
$6 \rightarrow 5$	1343 cm^{-1}	$\Sigma^+(00^00) \rightarrow \Sigma^+(02^00)$	Raman	1285.5	~ 60
		$\Sigma^+(00^00) \rightarrow \Sigma^+(10^00)$	very strong	1383.3	
		Fermi resonance			
$6 \rightarrow 4$	3814 cm^{-1}	$\Sigma_g^+(00^00) \rightarrow \Sigma_u^+(00^01)$	ir very strong	2349.3	~ 60
		$\Sigma_g^+(00^00) \rightarrow \Sigma_u^+(02^01)$	ir strong	3609	~ 60
		$\Sigma_g^+(00^00) \rightarrow \Sigma_u^+(10^01)$		3716	

$(D_{0,0,0}^{n_1,n_2,n_3})^2$ and a resonance function $I_{nn'}$ of ~ 100 cm^{-1} width:

$$\sigma_{n(0,0,0) \rightarrow n'(n_1 n_2, n_3)} \sim (D_{0,0,0}^{n_1,n_2,n_3})^2 I_{nn'}(\delta) .$$

IV. CONCLUSION

The laser-ablation technique developed in our laboratory has proven to be very efficient in producing a well-defined metal atomic beam. The pulsed nature of the beam allows the study of interaction of the metal atoms with reactive gas targets as long as the gas pressure is not too high. Furthermore, a combination of this technique with the pulsed-laser excitation technique, and a careful choice of the delay between the ablating laser and the probe laser, can be used to produce a beam of selectively excited atoms with relatively well-defined translation velocity. We have applied this novel technique to the study of l- and n-changing collisions between Li Rydberg states and CO_2.

Our results indicate that the l-mixing cross sections increase with n in the $n=5-13$ range. Our data complement those obtained previously by Higgs *et al.* for Xe and $n=25-37$,[13] where it was found that the cross section decreases with n. The whole set of data is relatively well described by the free-electron model of Hickman.[11] On this basis, a broad maximum of the l-mixing cross section is expected around $n=20-25$.

Finally, an interesting feature of the n-changing collisions is that large cross sections are obtained even when the change in electronic energy is quite large. This cannot be explained solely by nonresonant inelastic collisional processes. Several arguments, such as near energy coincidence with ir or Raman vibrational transitions of CO_2 and the resonance shape, support the proposed explanation of resonant-electronic to vibrational energy transfer.

ACKNOWLEDGMENTS

The groupe de Recherche sur l'Energétique des Milieux Ionisés is "Unité associée au Centre National de la Recherche Scientifique."

[1]L. Petitjean, F. Gounand, and P. R. Fournier, Phys. Rev. A **33**, 143 (1986); **33**, 1372 (1986), and references therein.
[2]B. Dubreuil and M. Harnafi, Phys. Rev. A **34**, 885 (1986).
[3]A. Kalamarides, L. N. Goeller, K. A. Smith, F. B. Dunning, M. Kimura, and N. F. Lane, Phys. Rev. A **36**, 3108 (1987).
[4]L. Petitjean and F. Gounand, Phys. Rev. A **30**, 2946 (1984).
[5]M. Harnafi and B. Dubreuil, Phys. Rev. A **31**, 1375 (1985).
[6]T. F. Gallagher, G. A. Ruff, and K. A. Safinya, Phys. Rev. A **22**, 843 (1980).
[7]M. Harnafi and B. Dubreuil, J. Phys. (Paris) Colloq. **48**, C7-677 (1987); M. Harnafi, T. Gibert, and B. Dubreuil, in Proceedings of the European Sectional Conference on the Atomic and Molecular Physics of Ionized Gases, Lisboa, 1988 [Europhys. Conf. Abstr. **12H**, 267 (1988)].
[8]P. Leismann, V. Henc-Bartolic, U. Rebban, H. J. Kunze, Phys. Scr. **30**, 530 (1984).
[9]R. W. Dreyfus, R. Kelly, R. E. Walkup, Appl. Phys. Lett. **49**, 1478 (1986).
[10]B. Dubreuil, in *Invited Papers of the XVIII ICPIG, Swansea, 1987* (Hilger, London, 1987), p. 302.
[11]A. P. Hickman, Phys. Rev. A **23**, 87 (1981).
[12]Y. Itikawa, At. Data Nucl. Data Tables **14**, 1 (1974).
[13]C. Higgs, K. A. Smith, F. B. Dunning, and R. F. Stebbings, J. Chem. Phys. **72**, 745 (1981).
[14]G. Herzberg, *Molecular Spectra and Molecular Structure Part II* (Van Nostrand, New York, 1945).

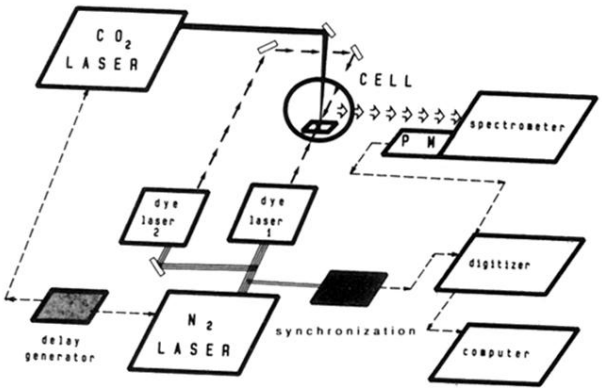

FIG. 1. Experimental setup.

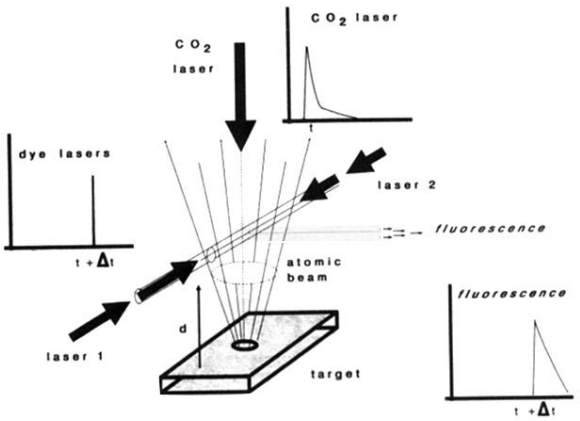

FIG. 2. Geometry of the laser–atomic-beam interaction. The CO_2 laser fired at time t is the ablating laser. Lasers 1 and 2 probe the atomic beam at the time $t+\Delta t$ and at a distance d from the surface. The resulting laser-induced fluorescence (LIF) is recorded.